Sensors & Diagnostics

PAPER

View Article Online
View Journal | View Issue

Cite this: *Sens. Diagn.*, 2024, **3**, 129

Colorimetric and dynamic light scattering dual-readout assay for formaldehyde detection based on the hybridization chain reaction and gold nanoparticles†

Wenxiu Huang,[a] Linyuan Chen,[a] Li Zou *[b] and Liansheng Ling *[a]

Formaldehyde (FA), as one of the largest indoor pollutants, can induce adverse health impacts and even cause various diseases. Therefore, it is necessary to establish a sensitive detection method for the determination of trace FA in the environment. Herein, a novel colorimetric and dynamic light scattering (DLS) dual-readout assay for FA detection is developed based on the hybridization chain reaction (HCR) and gold nanoparticles (AuNPs). In the presence of FA, Ag^+ ions bound by the DNA hairpin structure (HP) are reduced, and then the opened HP acts as an initiator to trigger the HCR process. The HCR products can induce the assembly of AuNPs *via* DNA hybridization, resulting in a sharp color change recorded using a smartphone camera and a significant increase in the diameter measured by DLS. The developed colorimetric sensor can detect FA as low as 20 μg L^{-1} through a smartphone application. Meanwhile, the DLS sensing strategy allows the determination of FA with a detection limit of 1.0 μg L^{-1}. Moreover, the proposed method shows excellent selectivity and acceptable applicability for the determination of FA in air, which might hold great application potential in environmental monitoring.

Received 1st August 2023,
Accepted 21st October 2023

DOI: 10.1039/d3sd00205e

rsc.li/sensors

Introduction

Formaldehyde (FA), a typical reactive carbonyl species (RCS), can be produced from plastics, furniture, cosmetics and medicine.[1,2] Meanwhile, FA is usually found from the residues of food such as vegetables, fruits and seafood because it can preserve freshness and enhance color.[3] According to the World Health Organization (WHO), the acceptable daily intake of FA is 0.15 mg per kg of body weight.[4] Previous studies have shown that excessive FA in the environment can cause various diseases, such as malformed embryos, heart disease, diabetes, neurodegenerative diseases and cancer.[5,6] Due to its damage to human health, FA has received much attention in recent decades. For instance, it was classified as a human carcinogen by the International Agency for Research on Cancer (IARC) in 2004.[7] To date, there have been some traditional methods for FA detection, such as high-performance liquid chromatography,[8] gas chromatography,[9] and selected ion flow tube-chemical ionization mass spectrometry.[10] Although these methods have high sensitivity and selectivity, most of them are limited by complicated sample preparation procedures, long measurement times and requirements for expensive equipment. Therefore, it is of great significance to develop novel methods for FA detection in the environment and living systems.

Au nanoparticles (AuNPs), one of the most commonly used nanomaterials, have been widely used in various kinds of analytical technology due to their unique optical properties, ease of synthesis and large surface areas.[11–13] In the past decades, AuNP-based sensors have seen significant applications in clinical diagnostics,[14] food analysis[15] and environmental monitoring.[16] However, the relatively poor sensitivity limits their wide applications to a certain extent. Recently, various nucleic acid amplification techniques have been employed in the development of AuNP-based sensors, such as polymerase chain reaction (PCR),[17] strand-displacement amplification (SDA),[18] rolling circle amplification (RCA),[19] catalytic hairpin assembly (CHA)[20] and hybridization chain reaction (HCR).[21] Among them, the HCR, an enzyme-free DNA amplification technology, has attracted considerable attention because of its efficient isothermal amplification capability.[22] For example, Zou *et al.* developed a novel colorimetric sensing strategy for the assay of acetylcholinesterase and donepezil in rat blood based on

[a] *School of Chemistry, Institute of Green Chemistry and Molecular Engineering, Sun Yat-Sen University, Guangzhou 510006, PR China.*
E-mail: cesllsh@mail.sysu.edu.cn
[b] *School of Pharmacy, Guangdong Pharmaceutical University, Guangzhou 510006, PR China. E-mail: lizou@gdpu.edu.cn*

† Electronic supplementary information (ESI) available. See DOI: https://doi.org/10.1039/d3sd00205e

Cu^{2+}-specific DNAzyme and HCR dual amplification coupled with the assembly of AuNPs.[23] Li *et al.* reported a sensitive AuNP-based dynamic light scattering (DLS) assay for non-invasive diagnosis of bladder cancer by detecting the telomerase activity in human urine using the HCR.[24] It is well known that AuNPs can not only serve as an excellent colorimetric signal reporter but also be used as DLS probes for biomedical analysis.[25] However, there is no report about the colorimetric/DLS detection of FA by using the HCR and AuNPs.

It is well-known that the cytosine–cytosine (C–C) mismatch DNA undergoes one key interaction involving complexation with Ag^+ ions.[26,27] In addition, highly selective sensors have been reported for the detection of small molecules, DNA, proteins, and metal ions by using Ag^+-mediated switchable DNA probes.[28–31] In parallel, FA, a highly reactive compound, can interact with the Ag^+ ions and induce them to form small particles and large aggregates.[32,33] According to the assumption above, a novel colorimetric and DLS dual-readout sensor for FA has been first developed based on the HCR and AuNPs. In this work, three DNA hairpin probes (HP, H1 and H2) are designed, the stem of HP contains two pairs of mismatched C–C for binding Ag^+. In the presence of FA, the hairpin structure of HP is opened, and then the HCR process can be triggered between H1 and H2. The obtained HCR products can hybridize with AuNP-oligo 1 probes, thereby resulting in aggregation of AuNPs, along with a concomitant color change from red to blue-purple and a significant increase in the diameter. Therefore, the determination of FA can be achieved by recording the RGB (red, blue, green) values of the sensing system using a smartphone application or measuring the particle size of AuNPs with a DLS instrument.

Experimental

Preparation of AuNP-oligo 1 probes

AuNPs were synthesized by a sodium citrate reduction method with an average diameter of 13 nm.[34] 1.0 mmol L^{-1} chloroauric acid (20 mL) was put into a round-bottom flask with a spherical condensing tube device, stirred in an oil bath and heated to 130 °C, and kept boiling at 130 °C for 30 min. Then, 2 mL of newly prepared sodium citrate solution was rapidly added to the round-bottom flask. The color of the solution gradually changed from light yellow to gray and then to wine red under continuous stirring at 130 °C for 15 min. The solution was then slowly cooled to room temperature under continuous agitation, filtered through a 450 nm nylon filter membrane, and stored in a refrigerator at 4 °C. AuNP-oligo 1 probes were prepared according to the literature.[35] Oligo 1 (5 OD) was dissolved in NaAc–HAc (pH 5.0, 10.0 mmol L^{-1}, 60 μL) and treated with TCEP (20.0 mmol L^{-1}, 12 μL) at room temperature for 1.5 h, and then mixed with 10 mL of AuNPs for 16 h. NaCl (2.0 mol L^{-1}, 530 μL) was added to the mixture in six separate increments over a period of 44 h, resulting in a final concentration of 0.1 mol L^{-1}. Finally, free oligonucleotides were removed by centrifugation 3 times (13 800 rpm, 30 min), and the resulting oil was precipitated in PBS buffer solution and stored in a refrigerator at 4 °C before use.

Polyacrylamide gel electrophoresis analysis

H1 and H2 were individually heated to 95 °C for 5 min, and then slowly cooled to room temperature to form a semi-stable hairpin structure. A mixture of H1 (10.0 μmol L^{-1}, 2 μL), H2 (10.0 μmol L^{-1}, 2 μL), HP (1.0 μmol L^{-1}, 4 μL) and PBS buffer (12 μL) was incubated at 25 °C for 1.0 h. The HCR products were characterized by polyacrylamide gel electrophoresis. 30% acrylamide/methyl-bisacrylamide solution (4.0 mL), ultra-pure water (3.0 mL), 5 × TBE buffer (1.0 mL), APS (0.1 g L^{-1},100 μL), and TEMED solution (4 μL) were successively added to make a gel. The HCR products (15 μL) were mixed with a 6 × loading buffer (3 μL), and then the mixture was injected into the combed hole of the gel. The gel was soaked in 0.5 × TBE buffer and electrophoresis was carried out at 120 V constant pressure for 85 min. After the electrophoresis, the gel was stained with 4S Red nucleic acid stain for 30 min, and the gel was photographed using a gel imaging analysis system to obtain electrophoretic images.

Procedure of the homogeneous assay

The mixture of HP (1.0 μmol L^{-1}, 4 μL) and $AgNO_3$ (5.0 μmol L^{-1}) was denatured at 95 °C for 5 min and cooled to room temperature to form a hairpin structure. After that, 20 μL of FA with diverse concentrations were added to the HP mixture solution at 25 °C for 1 h to perform HCR. Then, AuNP-oligo 1 probes (4.0 nmol L^{-1}, 30 μL) were added to the mixture and incubated at 25 °C for 1.0 h. Finally, the color changes of the solution were recorded on a smartphone, and the RGB values for each color were identified using a smartphone application (APP, color). The hydrodynamic diameter of AuNPs was measured by DLS at 25 °C with a scattering angle of 90°. DLS measurements were carried out in triplicate, and the reported diameter value was the average of three measurements.

Results and discussion

Principle of the colorimetric/DLS sensing strategy

A sensitive colorimetric and DLS dual-readout assay for FA detection has been developed based on the HCR and AuNPs, which is illustrated in Scheme 1. In the absence of FA, Ag^+ ions are bound by the DNA hairpin structure (HP) through C–Ag^+–C coordination. In this state, the HCR between H1 and H2 does not occur and the AuNP-oligo 1 probes maintain good dispersity in the solution. On the other hand, the presence of FA can extract the Ag^+ ions from the HP/Ag^+ complex, resulting in the opening of the HP hairpin structure. The opened HP can trigger the HCR process between H1 and H2 to form long nicked dsDNA, and the obtained HCR products can

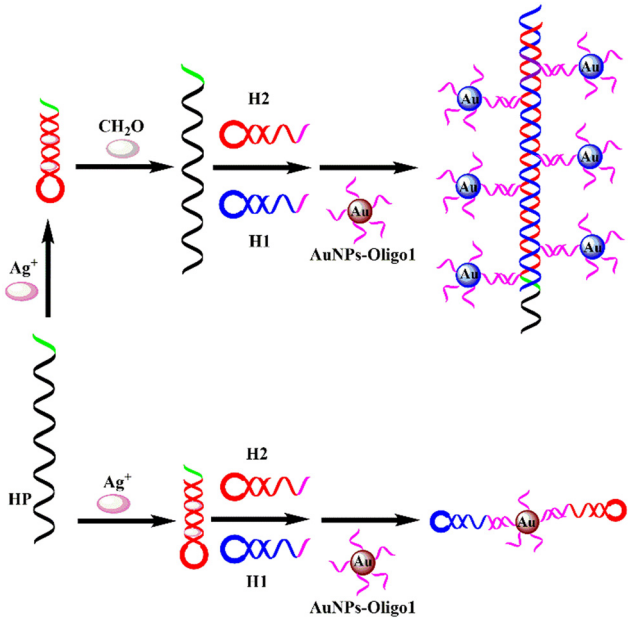

Scheme 1 Schematic illustration of the colorimetric and DLS dual-readout assay for FA detection.

hybridize with AuNP-oligo 1 probes, accompanied by the aggregation of AuNPs. As a result, a sharp color change from red to blue-purple can be recorded using a smartphone camera and a significant increase in the diameter can be measured by DLS. Ultimately, FA detection can be transformed into the RGB values of the sensing system using a smartphone application and the hydrodynamic diameter of AuNPs.

Feasibility of the proposed sensing strategy

In order to study the feasibility of this method, a series of proof-of-concept experiments were performed for FA detection. As shown in Fig. 1A, in the absence of FA, the solution is red, and the RGB values obtained by the smartphone are 139, 54, and 70, respectively. After the addition of FA, the color of the solution becomes blue-purple, and the RGB values are 101, 38, and 65, respectively. The corresponding UV-vis absorption spectra (Fig. 1B) show that the local surface plasmon resonance absorption peak of the AuNP solution is at 520 nm without FA, and the local surface plasmon resonance absorption peak of the AuNP solution shifts to 600 nm with the addition of FA. Moreover, the results of DLS show that the hydrodynamic diameter of AuNPs is about 61 nm without FA (Fig. 2A), but it increases to 461 nm with the addition of FA (Fig. 2B). Therefore, the colorimetric/DLS sensing strategy for sensitive detection of FA has certain feasibility.

Optimization of the experimental conditions

In order to obtain the best analytical performance, the HCR temperature and time were optimized. The effect of the HCR temperature on the hydrodynamic diameter of AuNPs is shown in Fig. 3A. The hydrodynamic diameter of AuNPs increased significantly with the increase of HCR temperature. When the HCR temperature exceeded 25 °C, the hydrodynamic diameter of AuNPs slowly decreased. Therefore, 25 °C was chosen as the HCR temperature. The effect of the HCR time on the hydrodynamic diameter of AuNPs is shown in Fig. 3B. With the extension of incubation time, HCR products were gradually generated, which promoted the aggregation of AuNPs and significantly increased the hydrodynamic diameter of AuNPs. The diameter reached a plateau when the reaction time was longer than 1.0 h, so 1.0 h was chosen as the HCR time.

The effect of the Ag^+ concentration on the experimental results was further studied. As shown in Fig. 3C, when the Ag^+ concentration was 5.0 μmol L^{-1}, the hydrodynamic diameter of AuNPs was the largest, which indicates that the appropriate concentration of Ag^+ can be reduced by FA, causing HP to fail to form a hairpin structure and triggering the HCR, resulting in the aggregation of AuNPs. Therefore, the optimal concentration of Ag^+ is 5.0 μmol L^{-1}. The aggregation time of AuNPs also affects the experimental results. As shown in Fig. 3D, the hydrodynamic diameter of AuNPs increased with the increase of the aggregation time of AuNPs ranging from 2.0 h to 4.0 h. When the aggregation time was longer than 4.0 h, the hydrodynamic diameter of AuNPs gradually decreased, indicating that the aggregation of AuNPs can be completed after 4.0 h. Therefore, 4.0 h was determined as the aggregation time of AuNPs.

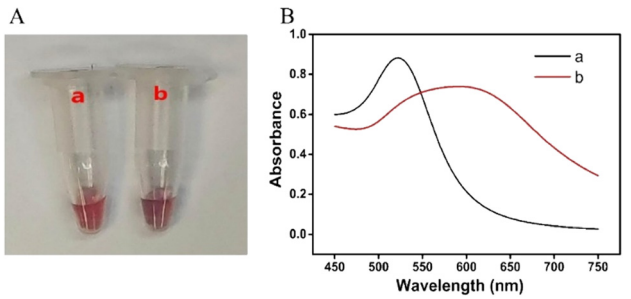

Fig. 1 Photograph (A) and UV-vis absorption spectra (B) of AuNP solution. (a) Ag^+ + HP + H1 + H2 + AuNP-oligo 1 probes; (b) a + FA.

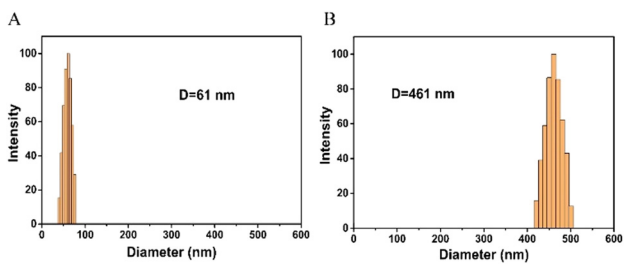

Fig. 2 Hydrodynamic diameter distribution of AuNP probes without (A) and with (B) addition of FA.

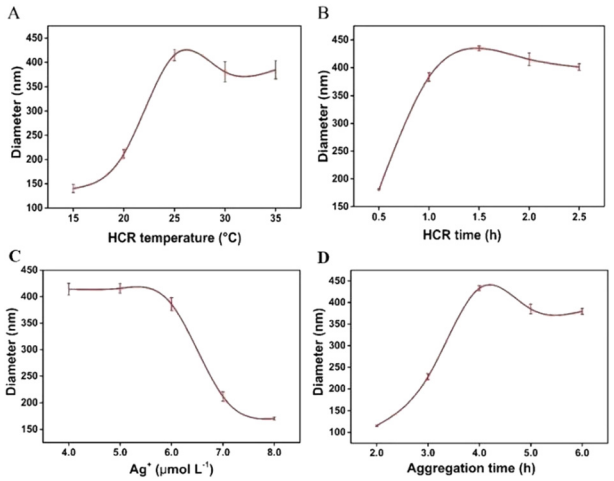

Fig. 3 Effects of (A) the HCR temperature, (B) the HCR time, (C) the concentration of Ag^+, and (D) the aggregation time of AuNPs on the performance of this assay. Error bars represent the standard deviation of three experiments.

Analytical performance for FA detection

Under the optimal experimental conditions, the analytical performance of the proposed sensing strategy was investigated by analysing different concentrations of FA. As shown in Fig. 4A, there is a good linear relationship between the *R*-value of the sensing system and the FA concentration in the range of 0.05 to 4.0 mg L^{-1}. The linear regression equation is $R = 167.8 - 20.05C$ (where R is the *R*-value and C is the formaldehyde concentration, respectively), with a correlation coefficient of $R = 0.9958$. The detection limit is calculated to be as low as 20 μg L^{-1} on the basis of 3σ/slope. Meanwhile, a good linear correlation between the hydrodynamic diameter and the FA concentration ranging from 2.0 μg L^{-1} to 4.0 mg L^{-1} is obtained (Fig. 4B), with a linear regression equation of $D = 61.49 + 102.16C$ (correlation coefficient $R = 0.9962$, where D is the hydrodynamic diameter of AuNPs and C is the formaldehyde concentration, respectively). A detection limit down to 1.0 μg L^{-1} is obtained, which is comparable or even superior to those of other methods for FA detection. Herein, the high sensitivity of the proposed sensor is derived from

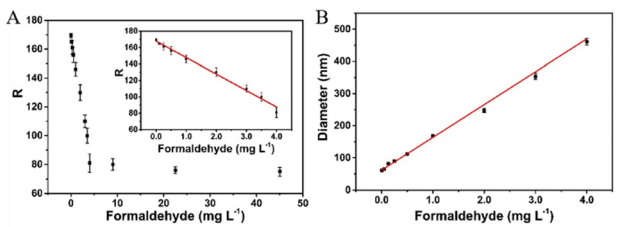

Fig. 4 (A) Plots of the *R*-value of the sensing system *versus* the concentration of FA. Inset shows the calibration curve for concentrations ranging from 0.05 to 4.0 mg L^{-1}. (B) Linear relationship of the hydrodynamic diameter of AuNPs *versus* the concentration of FA. The error bars indicate the standard deviations of three measurements.

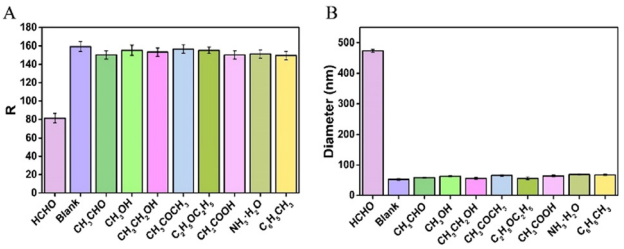

Fig. 5 (A) *R*-Value of the sensing system in the presence of different compounds; (B) diameter of AuNP probes in the presence of different compounds. The error bar represents the standard deviation of three duplicate samples.

the signal amplification of the HCR and the inherent advantage of the DLS technique.

To evaluate the selectivity of the proposed colorimetric/DLS sensor, some potential interferences including acetaldehyde, methanol, ethanol, acetone, ether, acetic acid, ammonia and toluene are individually added into the sensing system. As shown in Fig. 5A, the *R*-value of the sensing system containing the non-specific species is almost the same as that of the blank. However, a low *R*-value is obtained upon the addition of FA. Meanwhile, the diameter increases greatly compared to the background signal (blank) in the presence of FA (Fig. 5B). In contrast, no obvious enhanced signal is observed in the presence of other compounds. These results indicate that the proposed sensing strategy exhibited high specificity for FA.

Determination of FA in air

The active sampling method was used to recover the absorbent liquid from indoor air samples at Sun Yat-sen University. DLS was used to detect the absorbent solution of indoor air. The absorbent solution samples were spiked with different concentrations of FA and analyzed by the proposed method. As shown in Table 1, the obtained recoveries were in the range of 92.3 to 107% with relative standard deviations (RSD) less than 5.9%. These results show that the method has good accuracy and repeatability, and it is feasible to determine the concentration of FA in indoor air by this method. Since the absorption amount of gaseous FA in the aqueous solution is about 90%,[36] the FA concentration in air can be calculated according to the FA concentration in the absorbent solution. The concentration of FA in sample 2 is

Table 1 Detection of FA in indoor air ($n = 3$)

Sample	Added (mg L^{-1})	Found (mg L^{-1})	Recovery (%)	RSD (%)
1	0	0.03	—	5.6
	0.10	0.12	92.3	4.2
	0.50	0.51	96.2	5.2
	1.0	1.1	107	2.9
2	0	0.04	—	5.2
	0.10	0.13	92.9	3.3
	0.50	0.51	94.4	5.6
	1.0	1.1	106	5.9

0.04 mg L^{-1}, and the calculated FA concentration in air is 0.05 mg m^{-3}, which is less than the indoor FA concentration limit (0.1 mg m^{-3}) stipulated in the national standard, so the collected air samples meet the indoor air standard.

Conclusions

In summary, we have developed a novel colorimetric and DLS dual-readout sensor for sensitive detection of FA in air based on HCR signal amplification coupled with AuNPs. In the presence of FA, the HCR process is specifically triggered, which induces the aggregation of AuNPs, resulting in an obvious color change and a significant increase in the diameter. Owing to the excellent signal amplification ability of the HCR and the inherent advantage of the DLS technique, the sensitivity of the developed DLS sensor for FA detection is satisfactory, and the detection limit can reach as low as 1.0 μg L^{-1}. More interestingly, the RGB values of the sensing system can be identified using a smartphone application, which makes it an ideal format for on-site determination. In addition, this assay exhibits excellent selectivity and acceptable applicability for the detection of FA in air, showing great potential for environmental monitoring applications.

Author contributions

Wenxiu Huang: data curation, formal analysis, investigation, methodology, validation. Linyuan Chen: carried out part of experiments. Li Zou: visualization, funding acquisition, writing – original draft. Liansheng Ling: conceptualization, funding acquisition, project administration, resources, supervision, writing – review & editing.

Conflicts of interest

There are no conflicts to declare.

Acknowledgements

This work was supported by the National Natural Science Foundation of China (No. 22174166), the Natural Science Foundation of Guangdong Province (No. 2021A1515011519) and the Guangdong Provincial Medical Research Foundation (No. A2022473).

References

1 H. Ding, G. Yuan, L. Peng, L. Zhou and Q. Lin, *J. Agric. Food Chem.*, 2020, **68**, 3670–3677.
2 Y. Cao, Z. Teng, J. Zhang, T. Cao, J. Qian, J. Wang, W. Qin and H. Guo, *Sens. Actuators, B*, 2020, **320**, 128354.
3 N. Ding, Z. Li, Y. Hao and X. Yang, *Food Chem.*, 2022, **384**, 132426.
4 A. Bi, T. Gao, X. Cao, J. Dong, M. Liu, N. Ding, W. Liao and W. Zeng, *Sens. Actuators, B*, 2018, **255**, 3292–3297.
5 A. Roth, H. Li, C. Anorma and J. Chan, *J. Am. Chem. Soc.*, 2015, **137**, 10890–10893.
6 Y. Zhang, Y. Yang, X. He, P. Yang, T. Zong, P. Sun, R. Sun, T. Yu and Z. Jiang, *J. Cell. Mol. Med.*, 2021, **25**, 5358–5371.
7 G. M. Marsh, A. O. Youk and P. Morfeld, *Regul. Toxicol. Pharmacol.*, 2007, **47**, 59–67.
8 P. Wahed, M. A. Razzaq, S. Dharmapuri and M. Corrales, *Food Chem.*, 2016, **202**, 476–483.
9 A. Takeuchi, T. Takigawa, M. Abe, T. Kawai, Y. Endo, T. Yasugi, G. Endo and K. Ogino, *Bull. Environ. Contam. Toxicol.*, 2007, **79**, 1–4.
10 S. Kato, P. J. Burke, T. H. Koch and V. M. Bierbaum, *Anal. Chem.*, 2001, **73**, 2992–2997.
11 L. Zou and L. Ling, *Anal. Chem.*, 2018, **90**, 13373–13377.
12 H. Aldewachi, T. Chalati, M. N. Woodroofe, N. Bricklebank, B. Sharrack and P. Gardiner, *Nanoscale*, 2018, **10**, 18–33.
13 L. Zou, C. Mai, M. Li and Y. Lai, *Anal. Chim. Acta*, 2021, **1178**, 338804.
14 W. Zhou, X. Gao, D. Liu and X. Chen, *Chem. Rev.*, 2015, **115**, 10575–10636.
15 L. Zou, X. Li and Y. Lai, *Microchem. J.*, 2021, **162**, 105858.
16 K. Mao, H. Zhang, Z. Wang, H. Cao, K. Zhang, X. Li and Z. Yang, *Biosens. Bioelectron.*, 2020, **148**, 111785.
17 L. Zou, R. Shen, L. Ling and G. Li, *Anal. Chim. Acta*, 2018, **1038**, 105–111.
18 J. Wang, J. Zhang, T. Li, G. Li and L. Ling, *Biosens. Bioelectron.*, 2019, **131**, 143–148.
19 P. Wang, T. Zhang, T. Yang, N. Jin, Y. Zhao and A. Fan, *Analyst*, 2014, **139**, 3796–3803.
20 L. Zou, X. Li, J. Zhang and L. Ling, *Anal. Chem.*, 2020, **92**, 12656–12662.
21 Z. Li, X. Miao, Z. Cheng and P. Wang, *Sens. Actuators, B*, 2017, **243**, 731–737.
22 R. M. Dirks and N. A. Pierce, *Proc. Natl. Acad. Sci. U. S. A.*, 2004, **101**, 15275–15278.
23 L. Zou, X. Li, T. Li and L. Ling, *Sens. Actuators, B*, 2018, **267**, 272–278.
24 T. Li, L. Zou, J. Zhang, G. Li and L. Ling, *Anal. Chim. Acta*, 2019, **1065**, 90–97.
25 X. Liu, Q. Dai, L. Austin, J. Coutts, G. Knowles, J. Zou, H. Chen and Q. Huo, *J. Am. Chem. Soc.*, 2008, **130**, 2780–2782.
26 J. Li, H. Xi, C. Kong, Q. Liu and Z. Chen, *Anal. Chem.*, 2018, **90**, 11723–11727.
27 M. G. Wolfe, M. M. Ali and J. D. Brennan, *Anal. Chem.*, 2019, **91**, 4735–4740.
28 X. Jiang, W. Xu, X. Chen and Y. Liang, *Anal. Bioanal. Chem.*, 2019, **411**, 2439–2445.
29 J. S. Lee, P. A. Ulmann, M. S. Han and C. A. Mirkin, *Nano Lett.*, 2008, **8**, 529–533.
30 P. Chen, E. Sawyer, K. Sun, X. Zhang, C. Chen, B. Ying, X. Wei, Z. Wu and J. Geng, *Talanta*, 2019, **201**, 9–15.
31 J. Zhou, L. Han, Y. Ling, L. Wang, N. Li and H. Luo, *Talanta*, 2020, **219**, 121202.
32 L. Guo, H. Yin, M. Xu, Z. Zheng, X. Fang, R. Chong, Y. Zhou, L. Xu, Q. Xu, J. Li and H. Li, *ACS Sens.*, 2019, **4**, 2724–2729.

33 W. Yang, G. Zhang, J. Ni and Z. Lin, *Microchim. Acta*, 2020, **187**, 137.
34 J. J. Storhoff, R. Elghanian, R. C. Mucic, C. A. Mirkin and R. L. Letsinger, *J. Am. Chem. Soc.*, 1998, **120**, 1959–1964.
35 S. J. Hurst, A. K. R. Lytton-Jean and C. A. Mirkin, *Anal. Chem.*, 2006, **78**, 8313–8318.
36 M. Guglielmino, A. Allouch, C. A. Serra and C. S. Le, *Sens. Actuators, B*, 2017, **243**, 963–970.